

2018

**Experimental intravascular hemolysis induces hemodynamic and pathological pulmonary hypertension: association with accelerated purine metabolism**

Victor P. Bilan

Frank Schneider

Enrico M. Novelli

Eric E. Kelley

Sruti Shiva

*See next page for additional authors*

Follow this and additional works at: [https://researchrepository.wvu.edu/faculty\\_publications](https://researchrepository.wvu.edu/faculty_publications)



Part of the Allergy and Immunology Commons, Cardiology Commons, Critical Care Commons, Medical Biochemistry Commons, Medical Physiology Commons, Pathology Commons, Pharmacy and Pharmaceutical Sciences Commons, and the Pulmonology Commons

---

---

**Authors**

Victor P. Bilan, Frank Schneider, Enrico M. Novelli, Eric E. Kelley, Sruti Shiva, Mark T. Gladwin, Edwin K. Jackson, and Stevan P. Tofovic

---

# Experimental intravascular hemolysis induces hemodynamic and pathological pulmonary hypertension: association with accelerated purine metabolism

Victor P. Bilan<sup>1,2,3</sup>, Frank Schneider<sup>4</sup>, Enrico M. Novelli<sup>2,3</sup>, Eric E. Kelley<sup>5</sup>, Sruti Shiva<sup>2,6</sup>, Mark T. Gladwin<sup>1,2,3</sup>, Edwin K. Jackson<sup>6</sup> and Stevan P. Tofovic<sup>1,2,3</sup>

<sup>1</sup>Division of Pulmonary, Allergy and Critical Care Medicine, University of Pittsburgh School of Medicine, Pittsburgh, PA, USA; <sup>2</sup>Pittsburgh Heart, Lung and Blood Vascular Medicine Institute, University of Pittsburgh School of Medicine, Pittsburgh, PA, USA; <sup>3</sup>Department of Medicine, University of Pittsburgh School of Medicine, Pittsburgh, PA, USA; <sup>4</sup>Department of Pathology and Laboratory Medicine, Emory University School of Medicine, Atlanta, GA, USA; <sup>5</sup>Department of Physiology and Pharmacology, West Virginia University, Morgantown, WV, USA; <sup>6</sup>Department of Pharmacology and Chemical Biology, University of Pittsburgh School of Medicine, Pittsburgh, PA, USA

## Abstract

Pulmonary hypertension (PH) is emerging as a serious complication associated with hemolytic disorders, and plexiform lesions (PXL) have been reported in patients with sickle cell disease (SCD). We hypothesized that repetitive hemolysis per se induces PH and angioproliferative vasculopathy and evaluated a new mechanism for hemolysis-associated PH (HA-PH) that involves the release of adenosine deaminase (ADA) and purine nucleoside phosphorylase (PNP) from erythrocytes. In healthy rats, repetitive administration of hemolyzed autologous blood (HAB) for 10 days produced reversible pulmonary parenchymal injury and vascular remodeling and PH. Moreover, the combination of a single dose of Sugen-5416 (SU, 200 mg/kg) and 10-day HAB treatment resulted in severe and progressive obliterative PH and formation of PXL (Day 26, right ventricular peak systolic pressure (mmHg):  $26.1 \pm 1.1$ ,  $41.5 \pm 0.5$  and  $85.1 \pm 5.9$  in untreated, HAB treated and SU+HAB treated rats, respectively). In rats, repetitive administration of HAB increased plasma ADA activity and reduced urinary adenosine levels. Similarly, SCD patients had higher plasma ADA and PNP activity and accelerated adenosine, inosine, and guanosine metabolism than healthy controls. Our study provides evidence that hemolysis per se leads to the development of angioproliferative PH. We also report the development of a rat model of HA-PH that closely mimics pulmonary vasculopathy seen in patients with HA-PH. Finally, this study suggests that in hemolytic diseases released ADA and PNP may increase the risk of PH, likely by abolishing the vasoprotective effects of adenosine, inosine and guanosine. Further characterization of this new rat model of hemolysis-induced angioproliferative PH and additional studies of the role of purines metabolism in HA-PH are warranted.

## Keywords

pulmonary hypertension, hemolysis, sickle cell disease, purines, adenosine deaminase, purine nucleoside phosphorylase

Date received: 1 March 2018; accepted: 5 July 2018

Pulmonary Circulation 2018; 8(3) 1–15

DOI: 10.1177/2045894018791557

## Introduction

Recent progress in the care of patients with sickle cell disease (SCD) and other hemolytic diseases has resulted in significant improvements in both life expectancy and quality of life. However, as this new generation of patients ages, additional chronic complications associated with hemolytic diseases develop. Pulmonary hypertension (PH) is emerging as

Corresponding author:

Stevan P. Tofovic, Division of Pulmonary, Allergy and Critical Care Medicine, Vascular Medicine Institute, Department of Medicine, University of Pittsburgh School of Medicine, 100 Technology Drive, Room 542, Pittsburgh, PA 15219, USA.

Email: tofovic@pitt.edu



Creative Commons Non Commercial CC BY-NC: This article is distributed under the terms of the Creative Commons Attribution-NonCommercial 4.0 License (<http://www.creativecommons.org/licenses/by-nc/4.0/>) which permits non-commercial use, reproduction and distribution of the work without further permission provided the original work is attributed as specified on the SAGE and Open Access pages (<https://us.sagepub.com/en-us/nam/open-access-at-sage>).

© The Author(s) 2018.

Reprints and permissions:  
[sagepub.co.uk/journalsPermissions.nav](http://sagepub.co.uk/journalsPermissions.nav)  
[journals.sagepub.com/home/pul](http://journals.sagepub.com/home/pul)



the leading cause of morbidity and mortality in adult patients with various hemolytic disorders including SCD and thalassemia. Recent studies using right heart catheterization (a gold standard for the diagnosis of PH) showed 6–10% prevalence of PH in patients with SCD,<sup>1–3</sup> and 2.1% prevalence in those with thalassemia.<sup>4</sup> Because SCD and thalassemia are the most common monogenetic diseases worldwide (an estimated 400,000 children with these severe hemoglobinopathies are born each year, and 30 million persons have SCD worldwide),<sup>5</sup> hemolytic anemia represents a major emerging cause of PH. Further, although patients with hemolytic disorders, including those with SCD, develop less severe elevations of pulmonary arterial pressure than patients with idiopathic PH, PH is now identified as the single greatest risk factor for death in SCD.<sup>1–3,6,7</sup>

Although whether and how hemolytic diseases are causally related to PH is unknown, there is growing line of evidence that hemolysis and plasma free hemoglobin may be directly involved in the pathophysiology of proliferative vasculopathy and PH in hemolytic patients. For example, in a mouse model of SCD all animals develop PH even in the absence of in situ thrombosis or vaso-occlusive events.<sup>8</sup> Furthermore, in rats chronic hemoglobin infusion potentiates hypoxia-induced lung vascular oxidation, inflammation, remodeling and PH, and these effects are abolished or attenuated by haptoglobin therapy.<sup>9</sup> Patients with SCD who experience hyper-hemolysis have fewer vaso-occlusive crises, yet develop PH more frequently and die sooner than patients with less extensive hemolytic events.<sup>10</sup> These data suggest that hemolysis is mechanistically related to PH. However, the causal relationship between intravascular hemolysis and the development of PH remains controversial.<sup>11–13</sup>

Occlusive pulmonary vasculopathy and plexiform lesions (PXL) have been detected at autopsy in 25% to 60% of SCD patients.<sup>14,15</sup> However, the Berkeley mouse, the most commonly used experimental model of SCD, does not develop endothelial injury and pulmonary angioproliferative vasculopathy.<sup>16</sup> Similarly, in Sprague Dawley rats, chronic (7-week) infusion of hemoglobin induces PH and pulmonary vascular disease characterized by perivascular inflammation and media remodeling,<sup>17</sup> but absence of occlusive and plexiform lesions. Therefore, new experimental models are needed to investigate the underlying pathophysiology of hemolysis induced pulmonary vasculopathy and PH and to aid the development and evaluation of new therapeutic modalities.

In the present study, we used hemolyzed autologous blood (HAB) to determine whether hemolysis is mechanistically related to PH and pulmonary vasculopathy in rats. We also tested this hypothesis by employing a “second hit” approach to produce a rat model that more closely mimics pulmonary vascular lesions in patients with hemolytic disease. In this model, endothelial injury was induced by administration of the VEGF type-2 receptor antagonist

Sugen-5416 (SU; 3-(3,5-dimethyl-1H-pyrrole-2-ylmethylene)-1,3-dihydro-indol-2-one) and then animals were exposed to repetitive intravascular hemolysis.

In addition to being rich in hemoglobin and arginase, red blood cells (RBCs) are also richly endowed with adenosine deaminase (ADA) and purine nucleoside phosphorylase (PNP),<sup>18,19</sup> and therefore hemolysis would be expected to release significant amounts of ADA and PNP from injured RBCs into plasma. Both ADA and PNP are relatively small proteins,<sup>20,21</sup> and therefore these two key enzymes in purines metabolism can pass between endothelial cells, i.e., escape from the circulation, and reach the extracellular space and perivascular tissue. ADA converts adenosine to inosine,<sup>22</sup> and PNP converts inosine to hypoxanthine and guanosine to guanine.<sup>19</sup> Thereby, in diseases involving intravascular hemolysis, ADA and PNP should be expected to reduce extracellular adenosine, inosine and guanosine levels. Adenosine, inosine and guanosine induce myriad biological effects that in aggregate may produce vasoprotective and anti-occlusive effects and may reduce the risk for development of PH in SCD patients.<sup>22–31</sup> Therefore, in addition to testing the hypothesis that hemolysis can directly causes PH and pulmonary vasculopathy, we also investigated the changes in purine metabolism that may potentially be involved in hemolysis-induced vasculopathy and PH. In this regard, we examined whether in SCD patients chronic hemolysis is associated with release of ADA and PNP from RBCs, accelerated purine metabolism, and reduced extracellular levels of purines.

## Material and methods

### Animals

Male, 10–12 weeks old, Sprague Dawley rats were purchased from Charles River (Wilmington, MA), and were allowed to acclimatize for one week before inclusion into the study. The Institutional Animal Care and Use Committee approved all experimental protocols, and all experiments were conducted in accordance with the University of Pittsburgh guidelines for animal welfare.

**Protocol 1: HAB-induced pulmonary vasoconstriction and PH.** For acute administration of HAB, male Sprague Dawley rats were anesthetized with pentobarbital (45 mg/kg i.p.) and placed on a Deltaphase isothermal pad (Braintree Scientific, Braintree, MA) to maintain body temperature at  $37 \pm 0.5^\circ\text{C}$ . A PE-240 polyethylene catheter was inserted into the trachea to facilitate breathing, and a PE-50 catheter was inserted into the left carotid artery and connected to a digital blood pressure analyzer (BPA, Micro-Med. Inc., Louisville, KY) for continuous measurements of systolic, diastolic, and mean arterial blood pressure and heart rate. The left jugular vein was exposed and cannulated with a PE-50 catheter for delivery of HAB. Next, the right jugular

vein was exposed and a miniature pressure transducer catheter (SPR-513, Millar Instruments, Houston, TX) connected to a digital heart performance analyzer (Power Lab 400, AD Instruments, Colorado Springs, CO) was advanced into the right ventricle (RV) cavity via the right jugular vein and right atrium. A 30-min stabilization period was permitted before a 30-min HAB infusion (50  $\mu$ L/min) was initiated and 150-min recordings of right ventricular peak systolic pressure (RVSP) and systemic blood pressure were made. Two hours after completion of HAB infusion, urine samples were taken via bladder puncture for measurement of urinary ADA activity and adenosine and inosine concentrations. Urine ADA activity was measured by commercially available kit (Dyazyme Laboratories, Poway, CA).

For repetitive administration of HAB, male Sprague Dawley rats with a femoral vein indwelling catheter advanced to the entrance of the right atrium were purchased from Charles River (Wilmington, MA). On the day before initiating treatment, under isoflurane anesthesia, 1.5 mL of blood were withdrawn through the catheter, and after hematocrit was measured the sample was frozen and thawed three times. The next day, the 1.5 mL sampling procedure was repeated, and the previous day's HAB was infused for 15 min at a rate of 6 mL/kg/h. After 10 days of sampling and infusion, a subset of animals (HAB Day 10 group;  $n=8$ ) was anesthetized and instrumented for measurement of systemic blood pressure and closed-chest measurement of right ventricular function as described above. Hemodynamic measurements and blood and urine samples were collected 2 h after completion of the last HAB infusion. A subset of animals was allowed to recover from chronic hemolysis and was examined 16 days after last HAB infusion (HAB Day 26 group;  $n=8$ ). In control animals ( $n=6$ ) femoral vein indwelling catheter was flushed daily with 0.2 mL of saline containing 20% heparin. Urine adenosine and inosine levels after acute or repetitive hemolysis were measured by ultra-performance-tandem mass spectrometry as described in Protocol 4.

Animals were euthanized by overdose of anesthetic (pentobarbital, 200 mg/kg i.v.) and the heart and lungs were dissected and weighed. The RV free wall was separated from the left ventricle (LV) and the septum (S) and the Fulton index (RV/LV+S ratio) was calculated. The left bronchus was ligated and the left lung was stored at  $-80^{\circ}\text{C}$  and used for biochemical studies. The right lung was inflated and fixed with 10% buffered formalin at a height of 25 cm and immersed in formalin for at least 72 h before being embedded.

**Protocol 2: hemolysis-induced occlusive/angioproliferative PH.** Male Sprague Dawley rats with femoral vein indwelling catheters (Charles River, Wilmington, MA) were randomly assigned to one of the following three experimental groups: (1) control group – received vehicle (3 mL/kg, i.p.) and examined for pulmonary artery pressure and RV function after

26 days; (2) SU-Day 26 group – animals received VEGF receptor antagonist Sugen-5416 (SU; 200 mg/kg s.c. suspended in 0.5% (w/v) carboxymethyl cellulose) on Day 0 and examined on Day 26; and (3) SU+HAB group – animals received a single dose of SU on Day 0 and receiving HAB for 10 days, and examined on Day 26. At the end of the study, animals were instrumented for measurement of systemic and RV pressures as described in Protocol 1.

**Protocol 3: human samples collection and plasma ADA activity in pediatric SCD patients.** Blood samples were obtained from 20 pediatric patients with SCD (SS genotype,  $n=10$ , SC genotype,  $n=8$ ; S/ $\beta$  thalassemia,  $n=2$ ) and 12 age-matched healthy subjects and plasma samples generated according to the research protocols approved by the local institutional review board. Plasma samples were stored at  $-80^{\circ}\text{C}$  and later analyzed for plasma ADA activity. Briefly, after frozen plasma from each patient was thawed, two identical 0.4 mL aliquots were obtained from each sample, producing a sample pair. Adenosine (0.4 mL of a 3.5 mM solution) was added to each aliquot to give a final concentration of adenosine of 1.75 mM and to saturate ADA with respect to substrate. One aliquot of each sample pair was spiked with EHNA solution (20  $\mu$ L of a 200 mg/mL solution) to give a final EHNA concentration of 5 mg/mL. A 20  $\mu$ L of the vehicle for EHNA was added to the corresponding aliquot of each sample pair, and the samples were incubated at  $37^{\circ}\text{C}$  in a water bath. Next, 50  $\mu$ L portions were removed at 0, 15, 30, and 60 min after the beginning of the incubation. All 50  $\mu$ L portions were analyzed for adenosine content by HPLC with ultraviolet absorption, as described earlier.<sup>32</sup> The results from each patient were plotted (semi-logarithmic plot) as the amount of adenosine in sample versus time of incubation. The first-order rate constant for metabolism of adenosine by ADA was determined using linear regression.<sup>23</sup> The ADA activity was expressed as the difference of the first-order rate constants for disappearance of adenosine from plasma in the absence and presence of the ADA inhibitor EHNA ( $K_{\text{Basal}} - K_{\text{EHNA}}$ ;  $\text{min}^{-1}$ ). Urine samples were collected both in asymptomatic patients ( $n=8$ ) and in patients during a vaso-occlusive pain crisis ( $n=7$ ). In two patients, urine samples were collected both during periods of crisis and remission. Because cAMP may be an important source for adenosine biosynthesis, and to correct for variation in urine volume and collection efficiency, urinary adenosine concentrations were normalized by urine cAMP concentrations.

**Protocol 4: measurement of purines in adult SCD patients by mass spectrometry.** Spot urine samples were obtained from 11 adult asymptomatic SCD patients (8 male and 3 female;  $25.6 \pm 1.8$  y/o; Hb =  $9.96 \pm 0.64$ ; Htc =  $29.7 \pm 0.6\%$ ; reticulocytes =  $8.2 \pm 1.4\%$ ; LDH =  $295 \pm 15$  U/L) and five age-matched healthy controls. Urinary adenosine, inosine,

guanosine, guanine, hypoxanthine, xanthine, 8-aminoguanosine, 8-aminoguanine, and uric acid levels were measured by ultra-performance-tandem mass spectrometry in the selected ion monitoring mode, as previously described.<sup>33</sup>

#### Cell free plasma hemoglobin level measurement

Cell-free plasma hemoglobin was measured by conversion to cyano-methemoglobin with Drabkin's reagent and then by spectrophotometric measurement, as described previously.<sup>34</sup>

#### Measurement of radical formation

Freshly isolated lung tissue from control animals and rats treated with HAB were placed in Chelex-treated, ice-cold Krebs HEPES (KH) buffer (pH 7.4). Tissue was then cut into ~2 mm cubes (total of 50 mg wet weight) and placed into 100  $\mu$ L of ice cold KH buffer containing 200  $\mu$ M of the cell permeable spin probe CMH (cyclic hydroxylamine 1-hydroxy-3-methoxycarbonyl-2,2,5,5-tetramethyl-pyrrolidine) and 10  $\mu$ M deferoxamine. Samples were incubated for 30 min at 37°C and then 50  $\mu$ L of buffer was removed and analyzed for CM• radical formation using electron paramagnetic resonance (EPR) spectroscopy in a temperature and gas-controlled Bruker eScan table top EPR spectrometer. Samples were analyzed for 10 min at 37°C and 21% O<sub>2</sub>. Spectra represent five signal-averaged scans from  $t = 9$ –10 min. The EPR instrument settings were as follows: field sweep 50 G; microwave frequency 9.78 GHz; microwave power 20 mW; modulation amplitude 2 G; conversion time 327 ms; time constant 655 ms; and receiver gain  $1 \times 10^5$ .

#### Histopathology

Five-micrometer serial tissue sections from paraffin-embedded lungs were deparaffinized and stained with hematoxylin and eosin (H&E), pentachrome, and Verhoeff's Van Gieson (VVG) for histological and morphometric assessment. The Aperio ScanScope XT system (Aperio Inc., Vista, CA, USA) was used to scan entire glass slides at 20  $\times$  or 40  $\times$  magnification and Aperio Image Scope software was used to analyze digital slides.

Histopathological analysis of lung injury was performed on H&E slides by using a modified scoring system, as previously described.<sup>35, 36</sup> Five criteria were used to score lung injury: (i) infiltration or aggregation of inflammatory cells in alveolar spaces; (ii) hemorrhage (i.e., presence of RBCs or hemolyzed blood in alveolar spaces); (iii) edema; (iv) alveolar wall thickening; and (v) perivascular inflammation. Sections were scored as follows: 0, absent; 1, mild (<25% lung involvement); 2, moderate (25–50% lung involvement); 3, severe (50–75% lung involvement); 4, very severe (>75% lung involvement). Two serial slides were used and stained for H&E, pentachrome, or VVG stain. Between 65 and 115 small size pulmonary arteries (<50  $\mu$ M) per animal were analyzed for pulmonary vascular remodeling

(neomuscularization), incidence of occlusive vascular lesion, and presence of PXL and expressed as number of PXL per slide or normalized by number of examined small size arteries.

#### Immuno-spin trapping analyses of DNA radicals

To visualize *in situ* the extent of hemolysis-induced oxidation of lung tissue proteins, real-time trapping of biomolecular free radicals with the nitron spin trap 5,5-dimethyl-1-pyrroline-*N*-oxide (DMPO) was conducted. Twelve and six hours prior to single HAB infusion animals received DMPO (2g/kg, total, i.p.) and control animals received vehicle (saline, 2mL/kg i.p.). The presence of DMPO-adducted biomolecules in lung tissue taken 90 min after single HAB infusion was determined by using a primary rabbit polyclonal anti-DMPO antibody (Creative Diagnostics) followed by a goat anti-rabbit secondary anti-body.

#### Statistical analysis

All data are presented as mean  $\pm$  standard error of the mean. Statistical analysis was performed using the Number-Crunchers Statistical System software, and significance was defined as  $p < 0.05$ . Comparisons among multiple groups were performed by a one-factor analysis of variance (ANOVA). If this analysis indicated a significant difference among the means, multiple comparisons were made with a post-hoc Fisher's least significant difference test. A Student *t*-test was used to compare specific pairs of groups determined a priori to be of particular importance. A two-factor ANOVA was used to determine the effects of HAB and SU5416 and their interaction of development of progressive PH.

#### Results

In rats, a 30-min infusion of 1.5 mL of HAB into the right atrium resulted in prolonged vasoconstriction in the pulmonary and systemic circulation as evidenced by transient increases in RVPSP (Fig. 1(a)) and systemic mean blood pressure (MABP; Fig. 1(b)). Infusion of HAB induced marked increases in cell free hemoglobin (Fig. 1(c)) with maximal concentrations reached after completion of the infusion. Cell free hemoglobin decayed mono-exponentially with a half-life of 46 min and returned to baseline levels within 6 h (Fig. 1(d)). Single infusion of HAB was associated with significant generation of reactive oxygen species in the lung tissue as evidenced by EPR spectroscopy (Fig. 1(e)), and immuno-spin trapping analyses of biomolecular radicals (Fig. 1(f)), and significant lung sequestration of monocytes/macrophages (ED1+ cells; Fig. 1(g)). Finally, acute administration of HAB was associated with accelerated adenosine metabolism, augmented inosine production and increased ADA release/activity (Fig. 1(h)).

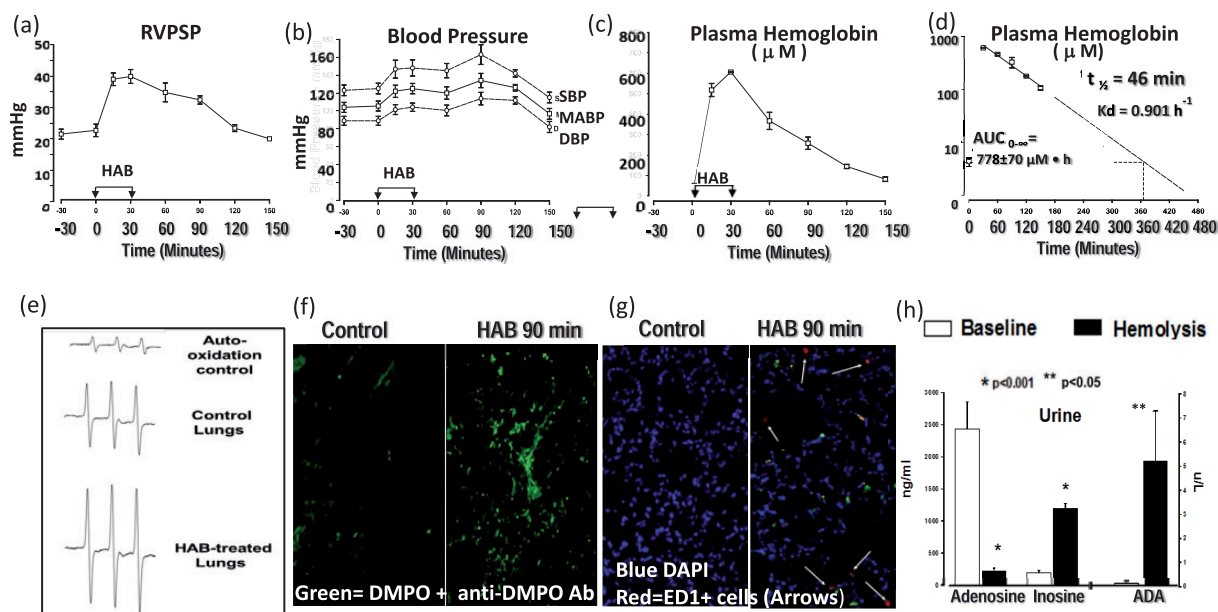


**Fig. 1.** Acute effects of HAB in male Sprague Dawley rats. HAB infusion (1.5 mL/30 min into right atrium;  $n = 6$ ) increases pulmonary (a) and systemic blood pressure (b). HAB infusion results in exposure of pulmonary circulation to plasma free hemoglobin up to 6 h (c, d). HAB infusion increases free radical formation in lung tissue (EPR spectra; lung tissue taken 90 min after completion of vehicle (control) or HAB infusion (e)). HAB infusion into the lungs induces biomolecular free radical generation in lung (green = DMPO) (f) and inflammatory cells sequestration (red = ED1 + cells; arrows) (g). Changes in urine adenosine and inosine levels and adenosine deaminase (ADA) activity before (baseline) and 60 min after administration of HAB indicate that hemolysis is associated with increased adenosine deaminase release and accelerated extracellular adenosine metabolism (h).

Chronic administration of 1.5 mL of HAB (that was taken from the same animal on the previous day and injected into the right atrium for 10 days) resulted in anemia, hemoglobinemia, splenomegaly, increased lung weight (Fig. 2(a) to (d)), PH, and isolated right ventricular hypertrophy (Fig. 2(e) and (f)), yet had no effect of liver weight (liver/b.w.:  $34.2 \pm 1.7$ ,  $38.2 \pm 1.49$ , and  $34.1 \pm 1.2$  g/kg body weight, control, HAB Day 10, and HAB Day 26 group, respectively). Repetitive hemolysis also increased systemic blood pressure (Fig. 2(g)) and was associated with accelerated adenosine metabolism and increased production of extracellular inosine (Fig. 2(h)) suggesting that repetitive hemolysis was associated with significant release of ADA from RBCs.

Plasma hemoglobin levels measured 2 h after the last HAB infusion on Day 10 (Fig. 2(b);  $144 \pm 10 \mu\text{M}$ ) were similar to free hemoglobin levels measured 2 h after a single HAB infusion (Fig. 1(c);  $125 \pm 17 \mu\text{M}$ ), suggesting no changes in hemoglobin clearance from plasma after repetitive hemolysis. Therefore, during chronic HAB administration, the pulmonary vascular bed was exposed to elevated plasma hemoglobin levels for only 6 h per day; yet this daily exposure of the pulmonary circulation to transient (up to 6 h) cell free hemoglobin insult was sufficient to induce moderate PH (Fig. 2(e)).

To determine whether repetitive hemolysis led to the development of reversible or progressive PH, a subset of rats was examined 16 days after completion of the 10-day

HAB treatment (Protocol 1, HAB-Day 26 group). In the HAB-Day 26 group, compared to control animals RVPSP and systemic blood pressure (Fig. 2(e) and (g)) and lung and spleen weights (Fig. 2(c) and (d)) were not elevated. Isolated RV hypertrophy, although reduced, was still present on Day 26 (Fig. 2(f)).

The histopathological analysis of lungs from animals that received 10-day HAB treatment revealed marked congestion and edema (Fig. 3(a)), hemorrhages (i.e., presence of hemolyzed blood and to smaller extent RBCs in the alveolar space; Fig. 3(b) and (c)), and marked alveolar wall thickening and perivascular inflammation (Fig. 3(c) and (d) and Fig. 4). At first sight, histological examination suggested that repetitive hemolysis induces significant media remodeling of small size pulmonary arteries (20–50  $\mu\text{m}$ ) (Fig. 3(d) and (e)). However, a thorough examination of VVG and pentachrome-stained lung sections revealed severe vasoconstriction of small vessels (50–100  $\mu\text{m}$ ; Fig. 3(f)) with only moderate “true remodeling” in the HAB-Day 10 group. Moderate media thickening that cannot be distinguished from mild-to-moderate vasoconstriction was also seen in medium sized arteries (100–300  $\mu\text{m}$ ; data not shown) which was usually associated with small bronchioles. One animal showed scattered fibrin thrombi in small vessels (Fig. 3(g)). Examination of VVG and pentachrome stained slides revealed no obliterative or angioproliferative changes in HAB-Day 10 group (data not shown).

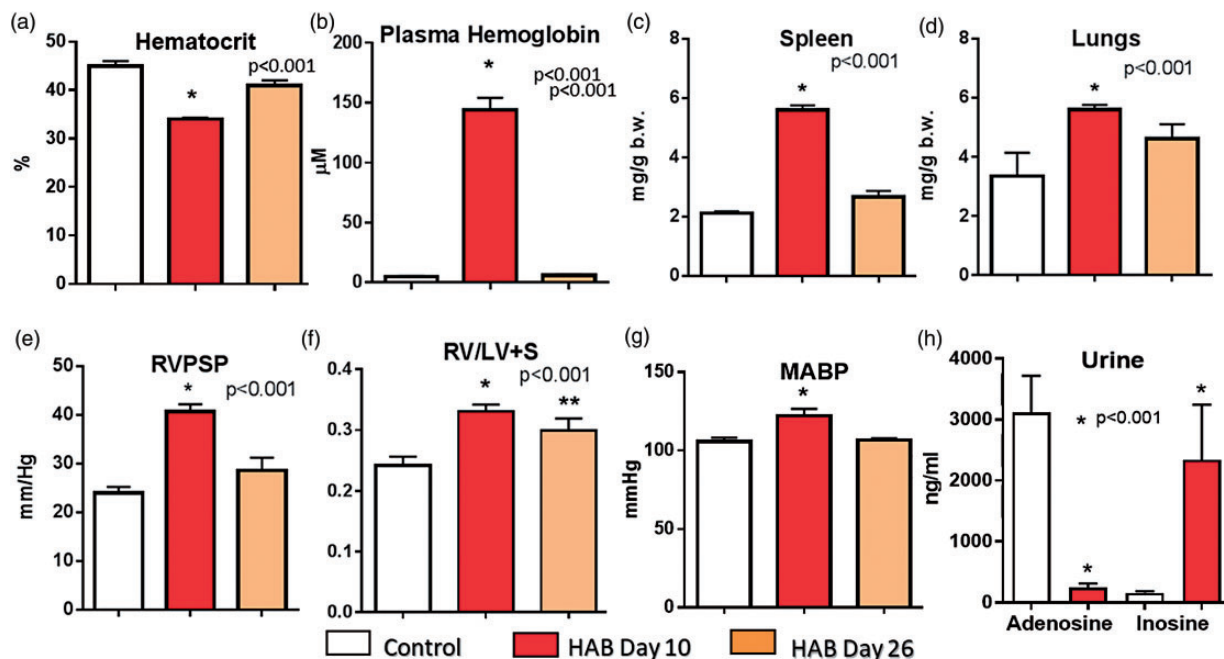


**Fig. 2.** The effects of repetitive administration of HAB (1.5 mL/30 min for 10 days; HAB Day 10 group;  $n = 8$ ). Some animals were examined 16 days after completion of 10-day HAB treatment (HAB Day 26 group;  $n = 7$ ). RVPSP and hematocrit were measured on Day 10 approximately 30 min before the last dose of HAB. Urine adenosine/inosine levels and plasma free hemoglobin were also measured on Day 10 approximately 2 h after administration of the last dose of HAB.

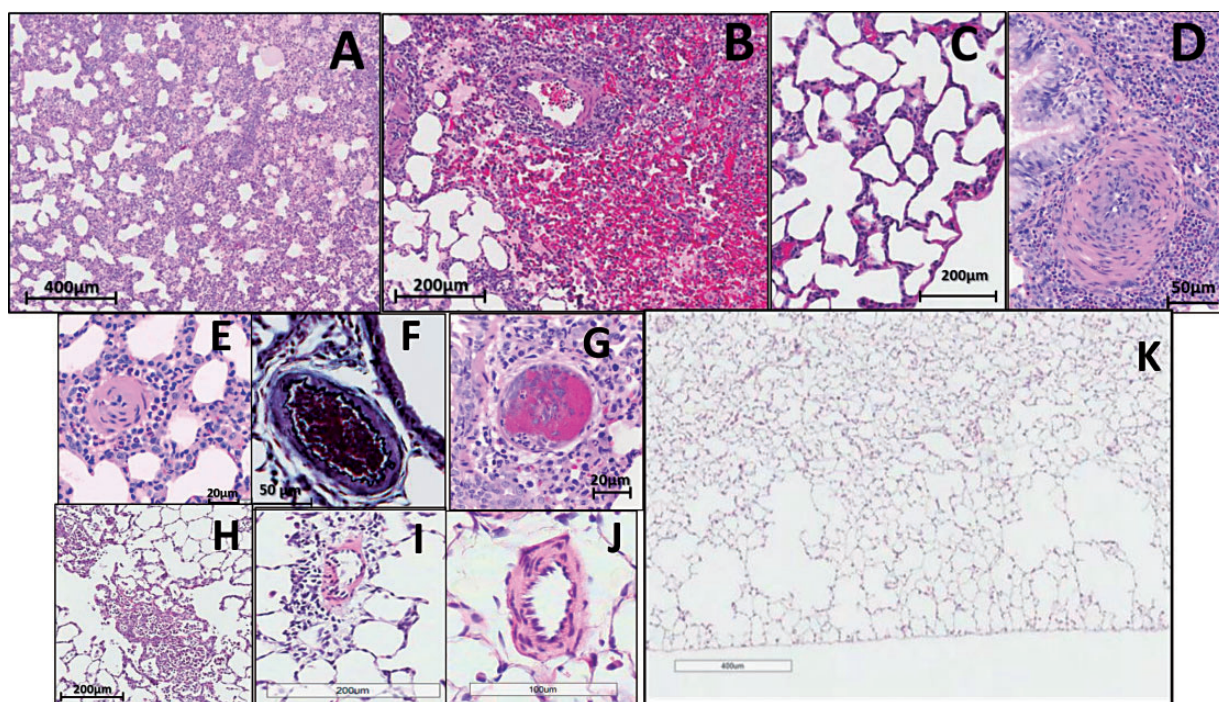


**Fig. 3.** Histopathological changes in rat lungs after 10 days of HAB administration (HAB Day 10 group;  $n = 8$ ). Chronic hemolysis induces congestion (a), hemorrhages (b), edema (a, b) alveolar thickening (c), perivascular inflammation (b, d, e), vasoconstriction of small pulmonary arteries (d, e). One out of eight animals showed scattered fibrin thrombi in small vessels (g). Although there was almost complete resolution of lung injury 16 days after completion of 10 days of HAB treatment, there remained emphysematous changes (k), sporadic parenchymal infiltrates (h), rare perivascular inflammation (i), and sporadic and mild vasoconstriction (j). (All images H&E stain, except for (f) which was VVG stain).



Sixteen days after completion of HAB treatment, histopathological analysis revealed near-normal lung histology in the HAB-Day 26 group as compared to control animals, with no-to-mild and sporadic congestion, perivascular lymphohistiocytic infiltration, and vascular remodeling (Fig. 3(h), (i), and (j), respectively). However, significant loss of alveolar septa, mainly in the peripheral lungs, was detected in animals from the HAB-Day 26 group that were allowed to recover from chronic hemolysis for 16 days (Fig. 3(k)).

Semi-quantitative analysis of lung injury and comparison between HAB Day 10 and HAB Day 26 groups (Fig. 4) confirmed the reversible nature of lung injury induced by 10-day HAB treatment and almost full recovery and resolution of lung changes 16 days after completion of HAB administration. Because repetitive hemolysis induced reversible pulmonary vascular injury, in the second set of experiments a “two-hit” approach was used. In this regard, animals were given a high-dose of Sugen 5416 (SU) and received a daily infusion of HAB for 10 days. We previously documented that high-dose SU (200 mg/kg/s.c.) attenuates the activity of VEGF type-2, but not VEGF type 1 receptors.<sup>37</sup> More importantly, we have shown that in combination with hypoxia a high-dose of SU induces within 3 weeks severe angioproliferative PAH and numerous PXL.<sup>37</sup> Furthermore, our preliminary experiments indicated that in the absence of hypoxia high-dose SU, but not the most commonly used low-dose (20 mg/kg), within a 6-week time frame produced similar and mild pulmonary vascular

injury and PH in both male and female rats.<sup>38</sup> We hypothesized that hemolysis superimposed on mild pulmonary vascular injury may lead to development of angioproliferative PH.

Indeed, the combination of inhibition of VEGF type-2 receptors with SU and repetitive hemolysis (10-day HAB administration) resulted in the development of severe and progressive PH (Fig. 5(a)). In some of the SU+HAB treated animals, RVSP pressures approached the values of systolic pressure in the systemic circulation. Notably, the SU+HAB combination induced severe RV hypertrophy (Fig. 5(b) and (c)) and significantly reduced RV contractility index (Fig. 5(d)) indicating ensuing RV failure. The SU+HAB treated animals were also hypertensive (Fig. 5(e)) and had increased heart, lung, and spleen weights (Fig. 5(f) to (h)). No significant changes in liver weight were detected (liver/b.w.:  $34.2 \pm 1.6$ ,  $34.6 \pm 1.1$ , and  $36.8 \pm 0.5$  g/kg, control, SU+HAB Day 26, and SU Day 26, respectively). The combination of hemolytic insult and VEGF type-2 receptor inhibition resulted in neomuscularization of small size pulmonary arteries (Fig. 6(b)) and induced occlusive angioproliferative lesions with more than 40% of examined vessels being partially or completely occluded (Fig. 6(a)). Disruption of the vascular elastic lamina with hypercellularity adjunct to the original vessel lumen was consistent with angioproliferative vasculopathy and on average six PXL per 100 examined vessels were detected (Fig. 6(c)). PXL in the SU+HAB Day 26 group (Fig. 6(d) to (f)) were similar to lesions seen in rats treated with SU (20 mg/kg) and exposed

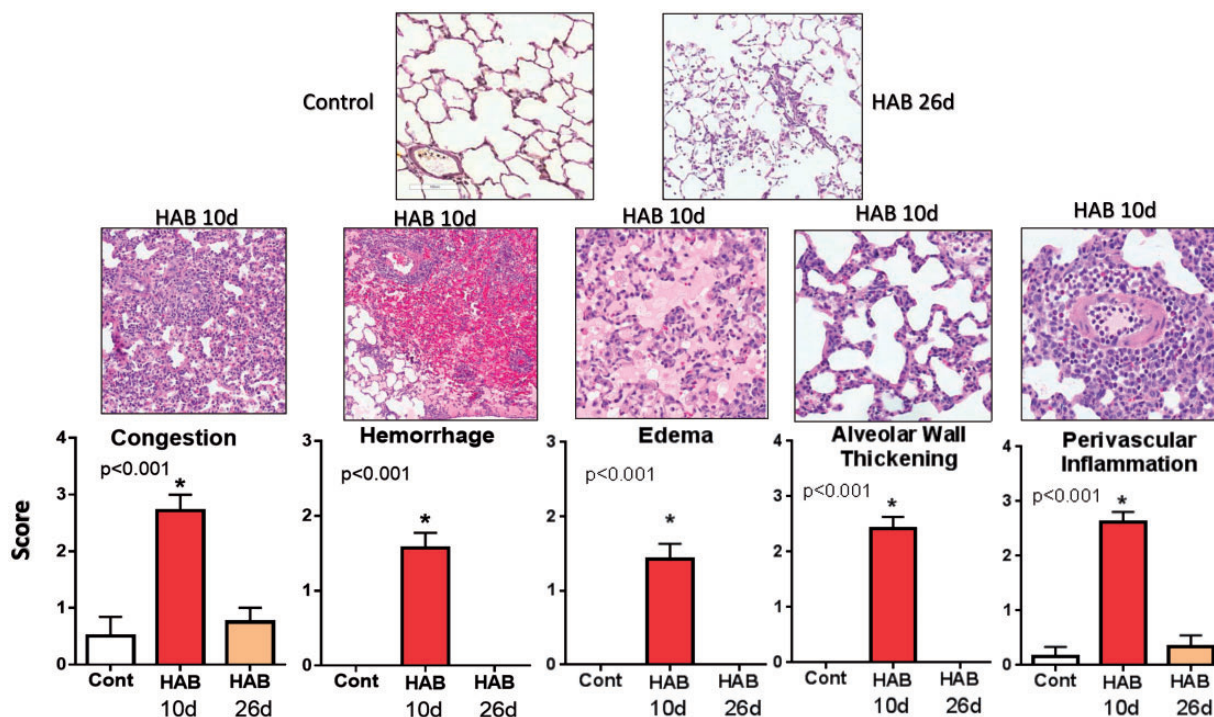


**Fig. 4.** Semi-quantitative assessment of pulmonary injury in control animals ( $n=6$ ), in rats after 10 days of HAB treatment (HAB Day 10 group;  $n=8$ ) and in animals examined 16 days after completion of HAB treatment (HAB Day 26 group;  $n=7$ ).

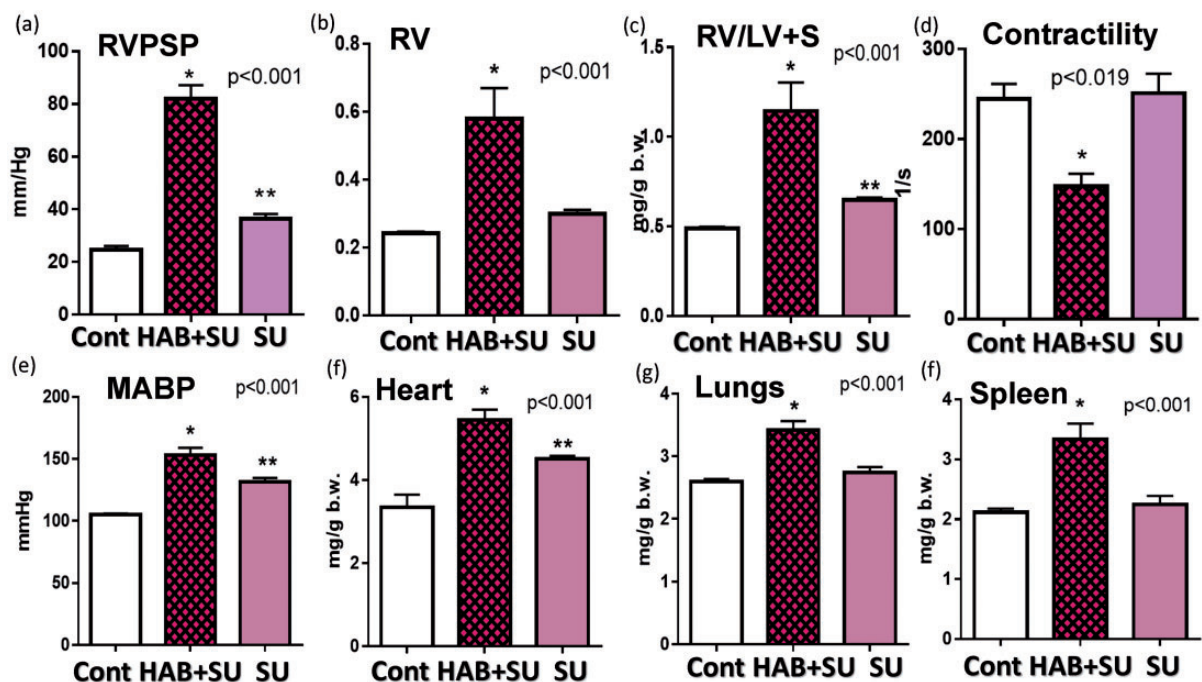


**Fig. 5.** The effects of VEGF type-2 receptor antagonist Sugen 5416 (SU 5416 Day 26) and the combination of Sugen 5416 + HAB (SU5416+HAB Day 26) on right ventricular (RV) peak systolic pressure (a), RV hypertrophy (b, c), RV contractility (d), mean arterial blood pressure (e), and organ weights (f-h). SU5416 + HAB rats develop progressive and severe PH. Sugen 5416 alone, induces mild PH, pulmonary vasoconstriction and mild-to-moderate vascular remodeling.

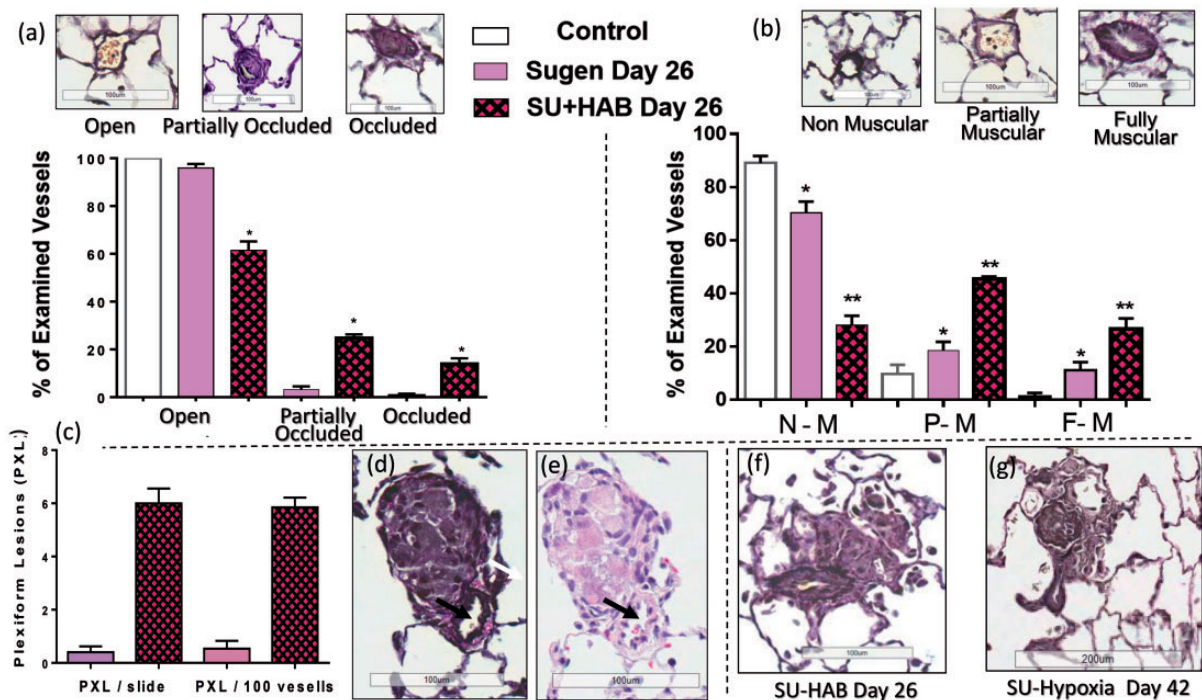


**Fig. 6.** Quantification of occlusive (a) and plexiform (PXL) lesions (c) and assessment of neomuscularization of small-size pulmonary arteries (b) in rats treated with either Sugen 5416 (SU Day 26 group;  $n = 8$ ) or the combination of Sugen 5416 + 10 days of HAB treatment (Group SU+HAB Day 26;  $n = 8$ ). The combination treatment resulted in development of numerous occlusive lesions in small-size ( $< 50 \mu\text{m}$ ) pulmonary arteries (a) and formation of PXL (d-f) similar to those seen in Sugen+hypoxia model (g).

to 3 weeks of hypoxia followed by 3 weeks of normoxia (Fig. 6(g)). Finally, media thickening of small-to-mid size pulmonary arteries with concentric (Fig. 7(a)) or asymmetric (Fig. 7(b)) remodeling was detected in the SU+HAB Day 26 group.

Administration of a high dose of SU alone increased blood pressure (Fig. 5(e)) and lung weight (Fig. 5(g)). At Day 26, the SU-Day 26 group had near normal histopathology with occlusive proliferative lesions detected in less than 2% of examined vessels and moderate medial remodeling in 5–10% of vessels (Fig. 6(a) and (b); Fig. 7(d) to (g)). Notably, compared with lungs from control animals, sections of lungs from the HAB Day 26 group had significant losses of alveolar septa and enlarged airspaces, suggesting emphysematous changes (Fig. 7(c)). This is consistent with a previous report that SU induces lung cell apoptosis and emphysema.<sup>39</sup> Surprisingly, although emphysematous changes were detected in rats treated with HAB or SU, such changes were not detected in the SU+HAB group. Analysis of emphysema development in rodents is challenging because its distribution is spatially heterogeneous. Because not all sections of the lung were sampled randomly, it is possible that because of the heterogeneity of the disease, we were not able to capture emphysematous changes in the SU+HAB group. Nonetheless, future characterization of the model should include quantification of emphysematous changes in all lung sections.

ADA activity in plasma samples from pediatric SCD patients and age-matched healthy controls are presented in Fig. 8. SCD patients had higher ADA activity than healthy controls (Fig. 8(a)). Importantly, plasma ADA activity was higher in patients with the SS genotype and in symptomatic (painful crisis) patients compared to heterozygous SCD and

asymptomatic patients, respectively (Fig. 8(d)). Plasma ADA activity inversely correlated with hemoglobin and hematocrit levels (Fig. 9(b) and (c)). Compared to asymptomatic patients, patients in painful crisis had reduced urinary adenosine levels (Fig. 8(e)), suggesting accelerated extracellular adenosine metabolism. Adult asymptomatic SCD patients also had increased urinary levels of inosine, hypoxanthine, xanthine and inosine/adenosine ratios compared to healthy controls, confirming the increased ADA activity and accelerated adenosine metabolism in SCD (Fig. 9(a) to (e)). Compared to urinary levels of inosine, the adult SCD patient had thirty times higher levels of hypoxanthine (inosine vs. hypoxanthine,  $\sim 1.1 \mu\text{g/mL}$  vs  $\sim 33 \mu\text{g/mL}$ ), suggesting increased release/activity of PNP. Adult SCD patients tended to have increased urinary guanosine levels (Fig. 9(f)) and had significantly increased guanine levels (Fig. 9(g)), further supporting the notion that hemolysis in SCD is associated with increased PNP release. Finally, SCD patients had reduced levels of 8-aminoguanosine and 8-aminoguanone, two endogenous inhibitors of PNP (Fig. 9(h) and (i)) which, at least in part, may explain the increased PNP activity in SCD.

## Discussion

In the present study, we used HAB to induce hemolytic vascular injury. A single dose of HAB induced a striking increase in cell free hemoglobin, marked pulmonary vasoconstriction, and systemic hypertension. Furthermore, a single dose of HAB induced severe oxidative stress and inflammatory responses in the lungs and was associated with increased extracellular ADA activity, accelerated adenosine metabolism, and increased levels of

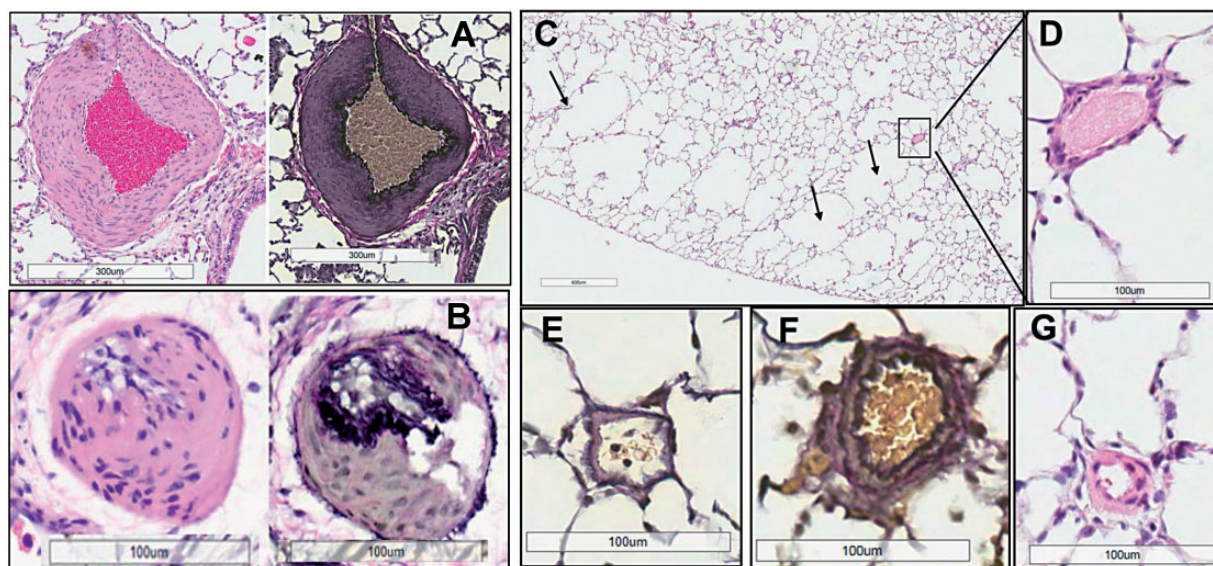


**Fig. 7.** Media thickening of small-to-mid size pulmonary arteries with concentric (a) or asymmetric (b) remodeling in SU+HAB treated rats on Day 26. Emphysematous changes (c) and near normal structure of small pulmonary arteries (d–g) 26 days after administration of Sugen 5416 (200 mg/kg).

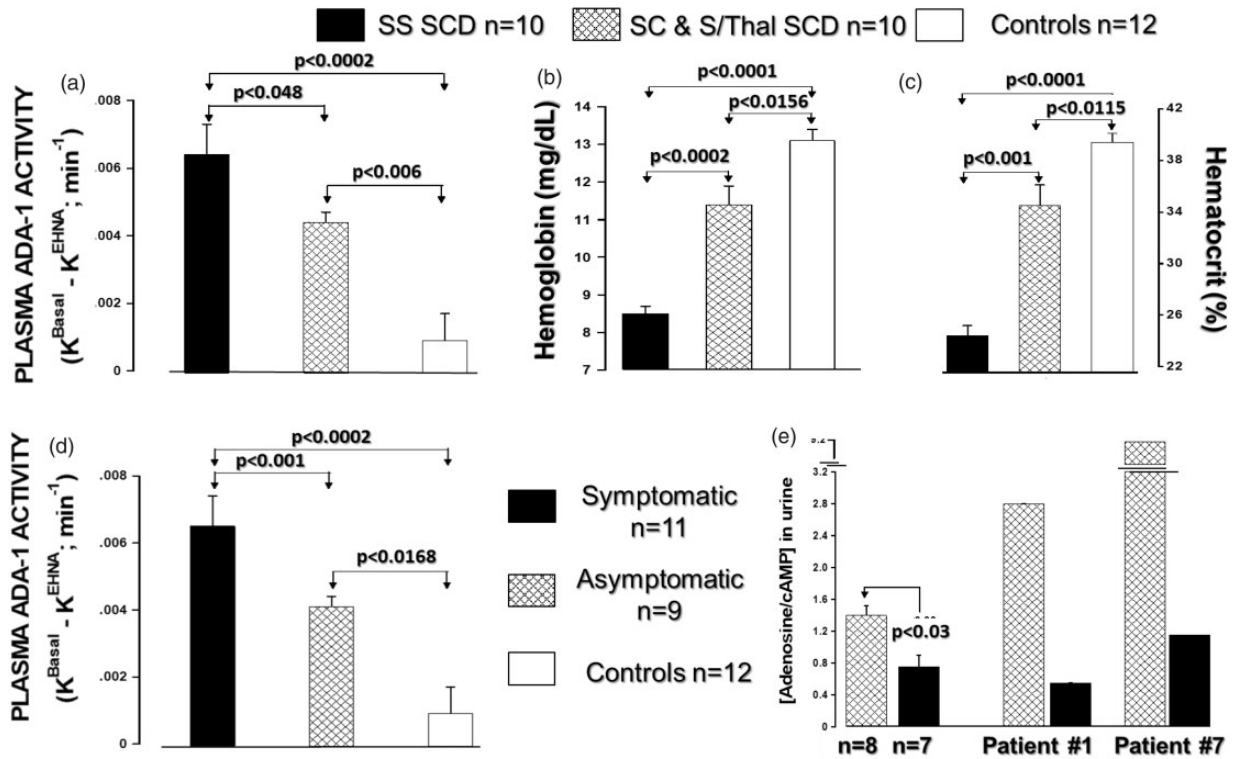


**Fig. 8.** Plasma adenosine deaminase (ADA) activity (a), hemoglobin (b) and hematocrit (c), and adenosine urine levels (e) in healthy subjects and pediatric patients with SCD. Plasma ADA activity is higher in patients with the SS genotype (a) and in symptomatic (painful crisis) patients (d) compared to heterozygote SCD and asymptomatic patients, respectively.

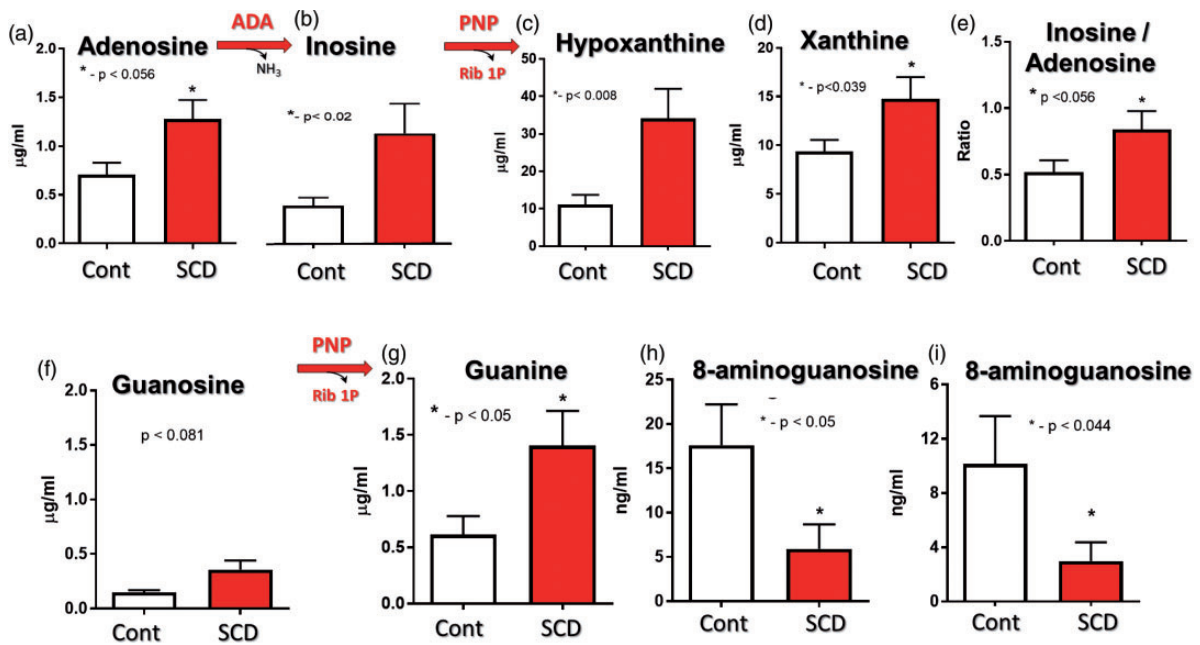


**Fig. 9.** Accelerated purine metabolism in adult asymptomatic SCD patients. Changes in urine adenosine (a) and inosine (b) levels and adenosine/inosine ratio (e) indicate increased extracellular ADA activity. Changes in inosine (b), hypoxanthine (c), guanosine (f) and guanine (g) levels indicate increased extracellular PNP activity. Hemolysis in SCD patient is associated with large production of vasculotoxic hypoxanthine (c) and xanthine (d). Reduced levels of endogenous PNP inhibitors 8-aminoguanosine (h) and 8-aminoguanine (i).

extracellular inosine. Plasma free hemoglobin was cleared from the circulation within 6 h after administration of HAB. Daily infusions of HAB delivered around 210 mg of hemoglobin per day, which is six times more than the daily doses of hemoglobin (35 mg/day over 7 weeks) shown to induce mild pulmonary vascular injury and moderate PH.<sup>17</sup> Yet, the total amount of intravascularly delivered hemoglobin was similar in both studies (~1700 mg over 7 weeks,<sup>17</sup> versus ~2200 mg over 10 days). HAB contains damage-associated molecular pattern molecules (DAMPs) that drive hemolytic vascular injury and inflammation and contribute to development of hemolytic vasculopathy and PH.<sup>40,41</sup> Therefore, it is not surprising that short-term (i.e., 10-day), intermittent (i.e., approximately 6 h per day) exposure to plasma free hemoglobin was sufficient to induce severe lung injury (Figs. 3 and 4) compared to very mild parenchymal and vascular lung injury seen with continuous infusion of low doses of hemoglobin (35 mg/day).<sup>17</sup> Severe lung injury in HAB treated rats included edema, hemorrhages, inflammatory infiltrates, congestion, perivascular inflammation, and alveolar thickening and pulmonary vascular injury in the form of severe vasoconstriction, perivascular inflammation and moderate PH.

In order to determine whether repetitive hemolysis induces permanent lung injury and progressive PH, some of the animals were examined 16 days after completion of the 10-day HAB treatment. Surprisingly, hemodynamic and histopathological analysis revealed that most of the hemolytic lung injury was resolved and moderate PH was reversed within a 16-day period. This suggests that the elevated pressure in the pulmonary circulation was primarily due to vasoconstriction rather than to “fixed PH” and irreversible vascular remodeling. Indeed, careful examination of vessels (VVG stain) showed relatively intact intima, and indicated that vessels with “media thickening” were actually markedly constricted, and mostly surrounded by significant inflammatory infiltrates. These findings also suggested that repetitive hemolysis, albeit for ten days, was not sufficient to induce permanent vascular changes and “fixed” PH.

There are two dominant histopathological features of SCD related to hemolytic pulmonary vasculopathy and PH (Group 5 PH): (1) marked obliterative pulmonary vascular remodeling in the form of thrombotic angiopathy with organizing and recanalized thromboemboli; and (2) occlusive endothelial cell proliferation and formation of PXL.<sup>15</sup> Surprisingly, in the current study, only one animal showed scattered fibrin thrombi in small vessels. Notably, in a rat model of pulmonary embolism, infusion of autologous clots induces transient (24-h) increases in pulmonary artery pressure, with near complete fibrinolysis of autologous pulmonary emboli within 5 days.<sup>42</sup> This may explain, at least in part, the resistance of rats to developing permanent hemolysis-induced lung and pulmonary vascular injury and thrombotic angiopathy. Whether longer (>10 days) exposure to hemolysis would result in thrombotic angiopathy in

our model is unknown and future studies should examine this possibility.

Proliferative vasculopathy and PXL at autopsy have been reported in 60% of SCD patients.<sup>14,15</sup> Yet, the most commonly used experimental model of SCD, the Berkeley mouse, does not develop significant endothelial vascular injury and pulmonary angioproliferative vasculopathy.<sup>16,17</sup> This precludes studies of hemolytic pulmonary vascular injury and PH in this model. Therefore, we used the “second hit” approach to produce a model that more closely mimics vascular lesions in humans. Endothelial injury was induced by the VEGF antagonist SU and subset of animals was exposed to repetitive hemolysis. SU alone induced systemic hypertension, moderate PH and mild-to-moderate vascular remodeling. This is consistent with our preliminary data that SU in a dose-dependent manner induces systemic hypertension and mild-to-moderate PH, pulmonary vasoconstriction, and mild vascular remodeling.<sup>38</sup> Notably, one SU treated animal was hemodynamically unstable and died before RV pressure measurements were taken. This animal developed significant vascular lesions that were characterized by endothelial cell proliferation, media hypertrophy, and disruption of the vascular elastic lamina in several small arteries (data not shown) and had marked RV hypertrophy (RV/LV+S: 0.577 vs.  $0.317 \pm 0.010$  for the rest of the SU Day 26 group). This finding indicates a variable response to SU per se in healthy, but outbred, Sprague Dawley rats. Furthermore, this finding suggests that VEGF inhibition per se (albeit in a small number of animals; 1 out of 6) may induce angioproliferative PH and warrants further investigation of the chronic effects of high- versus low-dose of SU on systemic and pulmonary artery pressure and pulmonary vascular structure.

In contrast to repetitive hemolysis alone that induced reversible and moderate PH, the “second hit” approach resulted in development of progressive and severe PH with occlusive angioproliferative vascular injury and formation of PXL. While hemolysis alone induced only moderate and reversible lung injury and PH with no signs of angioproliferative lesions, when hemolysis was superimposed on endothelial injury (i.e., SU treatment) severe, progressive, and angioproliferative PH occurred. This is similar to the “two-hit” SU+hypoxia model of PAH. Noteworthy, SU+HAB Day 26 rats develop similar PH (RVSP ~85 mmHg) and number of occlusive lesions (~15%) as rats treated with low-dose SU (20 mg) and exposed to hypoxia for 3 weeks followed by normoxia for 3 weeks. Furthermore, SU+HAB Day 26 rats develop similar PXL lesions compared to SU+hypoxia rats, albeit in smaller numbers (~5% vs 10%, SU+HAB vs. SU+hypoxia, respectively). Therefore, in our model, chronic hemolysis (i.e., HAB treatment) could be viewed as a substitute for chronic (3-week) hypoxia. In the current study, we did not measure blood oxygen saturation levels. Therefore, we cannot rule out the possibility that hypoxia (due to anemia and emphysematous changes) contributed to the

observed pulmonary vascular injury in HAB and SU+HAB treated rats. However, in SCD mice repeatedly exposed to 8% oxygen for 3 h, only a transient drop in SpO<sub>2</sub> occurred within the first hour of hypoxia that was associated with a dramatic increase in respiratory rate.<sup>43</sup> In contrast, daily HAB administration did not cause signs of distress, labored breathing, or tachypnea. Interestingly, normoxic activation of hypoxic responses (HIF-1 $\alpha$  and VEGF) has been reported in SCD patients and linked to development of PH in SCD.<sup>44</sup> The underlining mechanisms of the pathogenic effects of the hemolysis-SU interaction and hypoxic-pathway activation are unknown and deserve further investigation that should include correlation of markers of normoxic activation of hypoxic responses (HIF-1 $\alpha$  and VEGF) to changes in purine metabolism.

To the best of our knowledge this is the first model to exhibit hemolysis-induced angioproliferative lesions that more closely mimics pulmonary vascular changes seen in SCD patients. Noteworthy, whether PXL represent a by-standing morphologic marker of vascular injury or play a role in the pathogenesis and/or progression of PH has not yet been clarified. In this regard, published data in PAH patients,<sup>45</sup> and our preliminary data in female rats with accelerated and severe angioproliferative PAH,<sup>38</sup> suggest that the incidence of occlusive lesions, rather than the number of PXL, correlates with pulmonary artery pressure. Nonetheless, three-dimensional reconstruction studies suggest a topographical association of occlusive and plexiform lesions, with concentric occlusive lesions being present proximally to PXL.<sup>46</sup> PXL have a complex cellular composition that likely contributes to a micro-environment that is rich in angiogenic, proliferative, and inflammatory factors. Therefore, it is plausible that PXL may indirectly (i.e., via the induced micro-environment) contribute to increased pulmonary vascular resistance and remodeling and disease progression.

The initial characterization of our new rat model of hemolytic angioproliferative PH has several limitations. First, due to problems with patency of the jugular vein line, HAB was administered only for ten days. Therefore, it is possible that longer exposure to hemolysis alone would induce irreversible PH, thrombotic angiopathy, and parenchymal injury. Second, in addition to PH and RV dysfunction, cardiovascular manifestations of SCD also include both systolic and diastolic left ventricular dysfunction.<sup>47</sup> In the current study, the SU+HAB rats were evaluated within 26 day after initiation of treatments, and the long-term progressive character of angioproliferative PH and its impact on both right and left ventricle function were not addressed. Finally, for reasons explained in the Methods, we used a high dose of SU (200 mg/kg). This resulted in such severe PH that in some rats RVPSP levels were similar to the systemic blood pressure. This is in contrast to moderate, but deadly, PH seen in SCD patients. Therefore, further improvements of the model are warranted. This should include the use of low-dose SU in combination with

prolonged exposure to hemolysis, extended recovery, and measurement of RV and LV systolic and diastolic function and structure.

RBCs are rich in ADA and PNP,<sup>18,19</sup> and therefore during hemolysis significant alterations in purine metabolism would be expected. Indeed, previous studies indicate that hemolysis may be associated with increased release of ADA.<sup>22,48,49</sup> Therefore, in the present study we examined ADA and PNP activity and changes in purine metabolism in hemolysis-associated PH (HA-PH) rats and in pediatric and adult SCD patients. An important finding of this study is that in rats exposed to repetitive hemolysis and in patients with SCD, there is increased release of ADA from lysed RBCs, increased ADA plasma levels, and reduced extracellular adenosine levels. At present it is unknown whether, in addition to extracellular hemoglobin, the increased release of ADA and accelerated adenosine metabolism contribute to development of hemolytic vasculopathy and HA-PH. Nonetheless, based on well-defined biological effects of adenosine,<sup>22,50</sup> it is plausible that accelerated adenosine metabolism may have adverse effects in hemolytic vasculopathy and PH. In this regard, adenosine induces pulmonary vasodilation even under conditions of severe NO deficiency (i.e., conditions seen in patients with SCD and PH) and attenuates hypoxia-induced pulmonary inflammation.<sup>51</sup> In SCD mice, activation of A<sub>2A</sub> receptors improves baseline pulmonary function, reduces pulmonary inflammation, and prevents hypoxia-reoxygenation-induced exacerbation of pulmonary injury,<sup>52</sup> whereas genetic removal of A<sub>2A</sub> receptors in mice enhances pulmonary inflammation, confers PH, and increases pulmonary vascular remodeling.<sup>53</sup> Overall, these data are indicative of the potential adverse vascular effects of extracellular ADA in hemolytic vasculopathy. Countering these findings, a recent study suggests that adenosine signaling may have detrimental effects and that both ADA and reductions in extracellular adenosine levels produce beneficial effects in Berkeley mice with SCD.<sup>54</sup> However, the clinical significance of findings in SCD mice need to be confirmed in patients with SCD. Compared to human SCD, Berkeley SCD mice have more severe sickling and extravascular hemolysis;<sup>16</sup> and due to the longer plasma half-life of adenosine in mice, SCD mice have very high adenosine concentrations in the range of 7–8  $\mu$ M,<sup>54</sup> which are sufficient to activate low affinity A<sub>2B</sub> receptors. Yet, in SCD patients, much lower extracellular concentrations of adenosine (0.5  $\mu$ M) are detected.<sup>54</sup> This underscores the need for further studying adenosine metabolism and receptor signaling not only in SCD mice, but also in HA-PH rats and in patients with SCD.

Another important finding of this study is that in adult asymptomatic SCD patients there is increased release/activity of PNP and accelerated metabolism of two other purines, inosine and guanosine. This is accompanied by increased downstream production of vasculotoxic hypoxanthine and xanthine, and generation of reactive oxygen species, as evidenced by in vivo increased free radical production and

protein oxidation in HAB treated lungs. Notably, in ischemia/reperfusion injury (I/R) increased PNP release/activity in hepatic endothelial cells results in low inosine/guanosine levels and accumulation of hypoxanthine/xanthine, and correlates with  $O^{2-}$  production and poor liver function.<sup>55</sup> In contrast, both guanosine and inosine reduce I/R injury related oxidative/nitrosative stress. Guanosine, by inducing antioxidant enzyme heme oxygenase-1 (HO-1), inhibits the production of reactive oxygen species (ROS),<sup>24</sup> and prevents lipopolysaccharide-induced production of oxidative stress and inflammatory responses.<sup>23</sup> Noteworthy, pharmacologic or gene therapy augmentation of HO-1 activity provides protection against inflammation and vaso-occlusion in SCD mice.<sup>56,57</sup> Inosine also attenuates oxidative stress and related I/R end-organ damage.<sup>25,28–31</sup> Finally, platelet activation plays a significant role in vaso-occlusive crisis in SCD. It is significant, therefore, that guanosine and inosine exhibit anti-platelet effects. For example, these purines inhibit ADP-induced release of ATP, attenuate ADP- and collagen-induced platelet aggregation in vitro, delay platelet plugging and thrombus formation in vivo, and reduce platelet aggregation under arterial flow conditions.<sup>26–28</sup> The effects of PNP in hemolytic vasculopathy and PH are unknown. Yet, based on reported effects of inosine and guanosine and the present data, it is plausible that inhibition of PNP (i.e., inhibition of inosine and guanosine metabolism) may confer beneficial effects in hemolytic vasculopathy and PH. Notably, our preliminary data (presented at ATS 2018 annual meeting, Abstract B27:801) indicate that 8-aminoguanosine, a potent endogenous inhibitor of PNP, retards the progression of PAH and reduces angioproliferative lesions in female rats with SU+hypoxia-induced PH. Because RBCs are very rich in ADA and PNP, we consider ADA and PNP as important erythroid DAMPs that working in concert with extracellular hemoglobin (heme, iron) may exacerbate hemolytic vasculopathy and PH (Fig. 10).

Urinary purine analysis confirms previous reports and supports the notion that hemolysis is associated with ADA release and accelerated adenosine metabolism. Furthermore, for the first time, we report that SCD is associated with significant release of PNP and accelerated metabolism of guanosine and inosine. Yet, the initial characterization of the purine metabolome in SCD patients and our new rat model of hemolytic PH have several limitations. The presented data do not prove causation and it is not clear how changes in purine metabolism affect hemolytic vascular injury and PH. Furthermore, the effects of hemolysis and related PH on both right and left ventricle function and structure were not investigated. Therefore, future investigation of the purine metabolome in HA-PH rats, SCD mice, and SCD patients should include correlations of purines and their metabolites levels with (1) markers of hemolysis and normoxic activation of hypoxic responses, (2) actual or echocardiography estimated pulmonary artery pressure and cardiac output and (3) right and left ventricular function and structure. Finally, purine metabolism may be quite

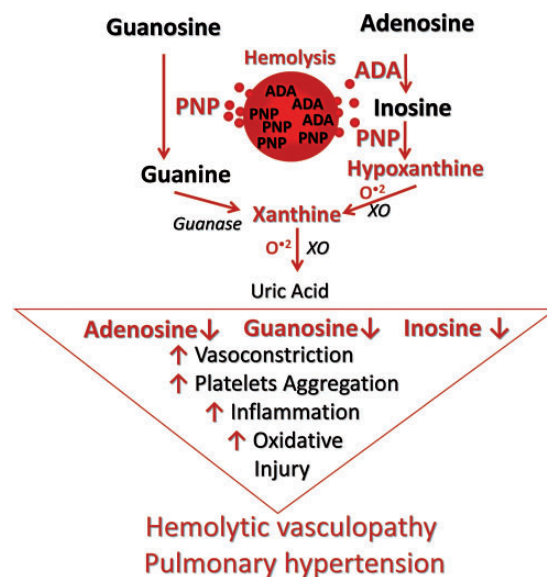


**Fig. 10.** Working hypothesis: erythroid DAMPs adenosine deaminase (ADA) and purine nucleoside phosphorylase (PNP) contribute to development/progression of hemolytic vasculopathy and PH.

different in rats and mice compared to SCD patients. Therefore, use of microdialysis techniques to measure plasma and extracellular purine levels in accessible tissues and organs (i.e., skeletal muscle, kidney, vascular lumen), should provide not only further insight into the role of the purine metabolome in hemolytic vasculopathy and PH, but also address the question of how data in rodents are relevant to hemolytic vasculopathy in SCD patients.

In summary, our study demonstrates that repetitive hemolysis induces PH. Moreover, we report the development of a rat model of hemolysis-induced PH that more closely mimics pulmonary vasculopathy seen in patients with chronic hemolysis associated PH. Repetitive hemolysis-induced PH is associated with increased extracellular ADA and PNP activity and altered adenosine, inosine, and guanosine metabolism. Further characterization of this new rat model of hemolysis-induced angioproliferative PH and additional studies of ADA and PNP activity and the purine metabolome in hemolysis-induced vasculopathy and PH are warranted.

#### Acknowledgments

Presented in part at American Thoracic Society meeting in San Francisco, May 2012.

#### Conflict of interest

The authors declare that there is no conflict of interest.

#### Funding

This work was supported in part by a P3HVBG grant from Vascular Medicine Institute, Hemophilia Center of Western Pennsylvania, and the Institute of Transfusion Medicine, Pittsburgh (SPT), and grants HL069846, HL109002, and DK079307 (EKJ).

## References

1. Fonseca GH, Souza R, Salemi VM, et al. Pulmonary hypertension diagnosed by right heart catheterisation in sickle cell disease. *Eur Respir J* 2012; 39: 112–118.
2. Mehari A, Gladwin MT, Tian X, et al. Mortality in adults with sickle cell disease and pulmonary hypertension. *JAMA* 2012; 307: 1254–1256.
3. Parent F, Bachir D, Inamo J, et al. A hemodynamic study of pulmonary hypertension in sickle cell disease. *N Engl J Med* 2011; 365: 44–53.
4. Derchi G, Galanello R, Bina P, et al. Prevalence and risk factors for pulmonary arterial hypertension in a large group of beta-thalassemia patients using right heart catheterization: a Webthal study. *Circulation* 2014; 129: 338–345.
5. Weatherall DJ. The inherited diseases of hemoglobin are an emerging global health burden. *Blood* 2010; 115: 4331–4336.
6. Castro O, Hoque M and Brown BD. Pulmonary hypertension in sickle cell disease: cardiac catheterization results and survival. *Blood* 2003; 101: 1257–1261.
7. Gladwin MT, Sachdev V, Jison ML, et al. Pulmonary hypertension as a risk factor for death in patients with sickle cell disease. *N Engl J Med* 2004; 350: 886–895.
8. Hsu LL, Champion HC, Campbell-Lee SA, et al. Hemolysis in sickle cell mice causes pulmonary hypertension due to global impairment in nitric oxide bioavailability. *Blood* 2007; 109: 3088–3098.
9. Irwin DC, Baek JH, Hassell K, et al. Hemoglobin-induced lung vascular oxidation, inflammation, and remodeling contribute to the progression of hypoxic pulmonary hypertension and is attenuated in rats with repeated-dose haptoglobin administration. *Free Radical Biol Med* 2015; 82: 50–62.
10. Taylor JG, Nolan VG, Mendelsohn L, et al. Chronic hyperhemolysis is sickle cell anemia: association of vascular complication and mortality with less frequent vasoocclusive pain. *PLoS One* 2008; 3: e2095.
11. Machado RF and Castro O. Sickle cell disease-associated pulmonary hypertension: overview of clinical manifestations and emerging therapeutic options. *Adv Pulm Hypertens* 2007; 6: 16–22.
12. Bunn HF, Nathan DG, Dover GJ, et al. Pulmonary hypertension and nitric oxide depletion in sickle cell disease. *Blood* 2010; 116: 687–692.
13. Gladwin MT. Revisiting the hyperhemolysis paradigm. *Blood* 2015; 126: 695–696.
14. Adedeji MO, Cespedes J, Allen K, et al. Pulmonary thrombotic arteriopathy in patients with sickle cell disease. *Arch Pathol Lab Med* 2001; 125: 1436–1441.
15. Haque AK, Gokhale S, Rampy BA, et al. Pulmonary hypertension in sickle cell hemoglobinopathy: a clinicopathologic study of 20 cases. *Hum Pathol* 2002; 33: 1037–1043.
16. Mancini EA, Hillery CA, Bodian CA, et al. Pathology of Berkeley sickle cell mice: similarities and differences with human sickle cell disease. *Blood* 2006; 107: 1651–1658.
17. Buehler PW, Baek JH, Lisk C, et al. Free hemoglobin induction of pulmonary vascular disease: evidence for an inflammatory mechanism. *Am J Physiol Lung Cell Mol Physiol* 2012; 303: L312–L326.
18. Geiger JD, Padua RA and Nagy JI. Adenosine deaminase regulation of purine actions. In: Phillis JW (ed.) *Adenosine and adenine nucleotides as regulators of cellular function*. Boca Raton FL: CRC Press, 1991, pp.71–84.
19. Bzowska A, Kulikowska E and Shugar D. Purine nucleoside phosphorylases: properties, functions, and clinical aspects. *Pharmacol Ther* 2000; 88: 349–425.
20. Shariff AJ, Wilson DK, Chang Z, et al. Refined 2.5 Å structure of murine adenosine deaminase at pH 6.0. *J Mol Biol* 1992; 226: 917–921.
21. Lewis AS and Lowy BA. Human erythrocyte purine nucleoside phosphorylase: molecular weight and physical properties. A Theorell-Chance catalytic mechanism. *J Biol Chem* 1979; 254: 9927–9932.
22. Tofovic SP, Jackson EK and Rafikova O. Adenosine deaminase-adenosine pathway in hemolysis-associated pulmonary hypertension. *Med Hypotheses* 2009; 72: 713–719.
23. Bellaver B, Souza DG, Bobermin LD, et al. Guanosine inhibits LPS-induced pro-inflammatory response and oxidative stress in hippocampal astrocytes through the heme oxygenase-1 pathway. *Purinergic Signall* 2015; 11: 571–580.
24. Dal-Cim T, Molz S, Egea J, et al. Guanosine protects human neuroblastoma SH-SY5Y cells against mitochondrial oxidative stress by inducing heme oxygenase-1 via PI3K/Akt/GSK-3beta pathway. *Neurochem Int* 2012; 61: 397–404.
25. Dowdall JF, Winter DC and Bouchier-Hayes DJ. Inosine modulates gut barrier dysfunction and end organ damage in a model of ischemia-reperfusion injury. *J Surg Res* 2002; 108: 61–68.
26. Fuentes E, Alarcon M, Astudillo L, et al. Protective mechanisms of guanosine from *Solanum lycopersicum* on agonist-induced platelet activation: role of sCD40L. *Molecules* 2013; 18: 8120–8135.
27. Fuentes E, Pereira J, Mezzano D, et al. Inhibition of platelet activation and thrombus formation by adenosine and inosine: studies on their relative contribution and molecular modeling. *PLoS One* 2014; 9: e112741.
28. Hsiao G, Lin KH, Chang Y, et al. Protective mechanisms of inosine in platelet activation and cerebral ischemic damage. *Arterioscler Thromb Vasc Biol* 2005; 25: 1998–2004.
29. Shen H, Chen GJ, Harvey BK, et al. Inosine reduces ischemic brain injury in rats. *Stroke* 2005; 36: 654–659.
30. Szabo G, Stumpf N, Radovits T, et al. Effects of inosine on reperfusion injury after heart transplantation. *Eur J Cardio-Thorac Surg* 2006; 30: 96–102.
31. Wakai A, Winter DC, Street JT, et al. Inosine attenuates tourniquet-induced skeletal muscle reperfusion injury. *J Surg Res* 2001; 99: 311–315.
32. Jackson EK, Mi Z, Koehler MT, et al. Injured erythrocytes release adenosine deaminase into the circulation. *J Pharmacol Exp Ther* 1996; 279: 1250–1260.
33. Ren J, Mi Z and Jackson EK. Assessment of nerve stimulation-induced release of purines from mouse kidneys by tandem mass spectrometry. *J Pharmacol Exp Ther* 2008; 325: 920–926.
34. MacArthur PH, Shiva S and Gladwin MT. Measurement of circulating nitrite and S-nitrosothiols by reductive chemiluminescence. *J Chromatogr B* 2007; 851: 93–105.
35. Wallace KL, Marshall MA, Ramos SI, et al. NKT cells mediate pulmonary inflammation and dysfunction in murine sickle cell disease through production of IFN-gamma and CXCR3 chemokines. *Blood* 2009; 114: 667–676.
36. Ghosh S, Adisa OA, Chappa P, et al. Extracellular hemin crisis triggers acute chest syndrome in sickle mice. *J Clin Invest* 2013; 123: 4809–4820.



37. Rafikova O, Rafikov R, Kumar S, et al. Bosentan inhibits oxidative and nitrosative stress and rescues occlusive pulmonary hypertension. *Free Radical Biol Med* 2013; 56: 28–43.
38. Tofovic SP, Bilan VP, Jackson EK, et al. Sugen 5416 dose-hypoxia-normoxia-gender interaction in angioproliferative pulmonary hypertension in rats. *Am J Respir Crit Care Med* 2014; 189: A5566.
39. Kasahara Y, Tudor RM, Taraseviciene-Stewart L, et al. Inhibition of VEGF receptors causes lung cell apoptosis and emphysema. *J Clin Invest* 2000; 106: 1311–1319.
40. Gladwin MT and Ofori-Acquah SF. Erythroid DAMPs drive inflammation in SCD. *Blood* 2014; 123: 3689–3690.
41. Mendonca R, Silveira AA and Conran N. Red cell DAMPs and inflammation. *Inflammation Res* 2016; 65: 665–678.
42. Runyon MS, Gellar MA, Sanapareddy N, et al. Development and comparison of a minimally-invasive model of autologous clot pulmonary embolism in Sprague-Dawley and Copenhagen rats. *Thromb J* 2010; 8: 3.
43. Tan F, Ghosh S, Mosunjac M, et al. Diametric effects of hypoxia on pathophysiology of sickle cell disease in a murine model. *Exp Biol Med* 2016; 241: 766–771.
44. Zhang X, Zhang W, Ma SF, et al. Hypoxic response contributes to altered gene expression and precapillary pulmonary hypertension in patients with sickle cell disease. *Circulation* 2014; 129: 1650–1658.
45. Stacher E, Graham BB, Hunt JM, et al. Modern age pathology of pulmonary arterial hypertension. *Am J Respir Crit Care Med* 2012; 186: 261–272.
46. Cool CD, Stewart JS, Werahera P, et al. Three-dimensional reconstruction of pulmonary arteries in plexiform pulmonary hypertension using cell-specific markers. Evidence for a dynamic and heterogeneous process of pulmonary endothelial cell growth. *Am J Pathol* 1999; 155: 411–419.
47. Voskaridou E, Christoulas D and Terpos E. Sickle-cell disease and the heart: review of the current literature. *Br J Haematol* 2012; 157: 664–673.
48. Jackson EK, Koehler M, Mi Z, et al. Possible role of adenosine deaminase in vaso-occlusive diseases. *J Hypertens* 1996; 14: 19–29.
49. Tofovic SP, Kusaka H, Li P, et al. Effects of adenosine deaminase inhibition on blood pressure in old spontaneously hypertensive rats. *Clin Exp Hypertens* 1998; 20: 329–344.
50. Idzko M, Ferrari D, Riegel AK, et al. Extracellular nucleotide and nucleoside signaling in vascular and blood disease. *Blood* 2014; 124: 1029–1037.
51. Khoury J, Ibla JC, Neish AS, et al. Antiinflammatory adaptation to hypoxia through adenosine-mediated cullin-1 deneddylation. *J Clin Invest* 2007; 117: 703–711.
52. Wallace KL and Linden J. Adenosine A2A receptors induced on iNKT and NK cells reduce pulmonary inflammation and injury in mice with sickle cell disease. *Blood* 2010; 116: 5010–5020.
53. Xu MH, Gong YS, Su MS, et al. Absence of the adenosine A2A receptor confers pulmonary arterial hypertension and increased pulmonary vascular remodeling in mice. *J Vasc Res* 2011; 48: 171–183.
54. Zhang Y, Dai Y, Wen J, et al. Detrimental effects of adenosine signaling in sickle cell disease. *Nat Med* 2011; 17: 79–86.
55. Rao PN, Walsh TR, Makowka L, et al. Purine nucleoside phosphorylase: a new marker for free oxygen radical injury to the endothelial cell. *Hepatology* 1990; 11: 193–198.
56. Belcher JD, Mahaseth H, Welch TE, et al. Heme oxygenase-1 is a modulator of inflammation and vaso-occlusion in transgenic sickle mice. *J Clin Invest* 2006; 116: 808–816.
57. Belcher JD, Vineyard JV, Bruzzone CM, et al. Heme oxygenase-1 gene delivery by Sleeping Beauty inhibits vascular stasis in a murine model of sickle cell disease. *J Mol Med* 2010; 88: 665–675.